



A Zn-Offretite for the adsorption of thiophenic species under fluidized catalytic cracking conditions. Synthesis, characterization and reactivity



Yira Aponte, Hugo de Lasa *

Chemical Reactor Engineering Centre, Faculty of Engineering Science, University of Western Ontario, London, ON N6A 5B9, Canada

ARTICLE INFO

Article history:

Received 2 December 2015
Received in revised form 5 February 2016
Accepted 14 February 2016
Available online 16 February 2016

Keywords:

Offretite
OFF
Zn-offretite
Sulfur adsorption
Zn-OFF zeolite
FCC additive
Zinc direct zeolite synthesis

ABSTRACT

A zinc-containing offretite (Zn-OFF) was synthesized using a hydrothermal method. The goal was to prepare a Zn-OFF zeolite with adsorption properties for selective removal of thiophenic chemical species in gasoline. It was expected that this new sorbent would perform favorably under the conditions close to the ones of FCC units. Following the Zn-OFF synthesis, several characterization techniques were used such as: a) temperature programmed desorption (TPD), b) temperature programmed reduction (TPR), c) temperature programmed oxidation (TPO), d) X-ray diffraction, e) N_2 isotherm, f) UV-vis spectra, g) Scanning Electron Microscopy (SEM) and h) Fourier Transform Infrared Spectroscopy (FTIR). In addition, chemical characterization was developed using Inductively Coupled Plasma Atomic Emission Spectrometry (ICP-AES) and X-Ray Fluorescence (XRF). It was proven on this basis, that zinc species are most likely included in the zeolite framework. Regarding the influence of Zn on the OFF zeolites, it was shown that Zn considerably increases (doubles) the weak acidity measured by TPD as well as shifts the TPD peak towards a higher temperature range. Additionally, FTIR pyridine adsorption also showed in the case of the Zn-OFF in comparison with the OFF, a 2.5 times higher abundance of Lewis acid sites versus Brønsted sites. It is speculated on this basis, that the Zn in the OFF structure increases species adsorption, changing the adsorption bonding strengths. Regarding the Zn-OFF performance, it was proven in a CREC Riser Simulator unit that one can achieve 37 wt% of 2-methylthiophene removal with less than 1.3 wt% being converted into coke.

© 2016 Elsevier B.V. All rights reserved.

1. Introduction

Offretite (OFF) zeolite synthesis methods have been studied by several authors. For example, Howden [1,2] found that the use of a tetramethylammonium (TMA) template is required for offretite synthesis. This is useful to avoid erionite zeolite formation. In addition, other authors proposed other methods for the OFF synthesis using other templates, cations as well as silicate sources [3–6].

In addition, researchers have also focused on the stabilization of the OFF via dealumination, which yields OFF zeolites with an increased stability and pore volume [7,8]. Most recently, an optimization of the synthesis of high pure OFF was achieved by Wang et al. [9] via magadiite recrystallization. In addition, Itakura et al. [10] claimed to have developed a method to obtain a highly thermally stable OFF by the hydrothermal conversion of faujasite.

There are however, only few catalytic studies where OFF zeolites are used. Examples of the OFF applications can be found in the conversion of toluene and in the isomerization of m-xylene [11,12]. These authors reported high isomerization activity. In addition, and for methanol conversion, a protonic offretite (H-OFF) was considered by Dejaive et al. [13]. It was found that coke is formed essentially in the larger pores (12 rings: $6.7 \times 6.8 \text{ \AA}$) leaving the active acid sites in the smaller pores (8 rings: $3.9 \times 4.9 \text{ \AA}$) freely accessible to reactant species. A similar conclusion was obtained by Bourdillon et al. [14], who evaluated the *n*-hexane and xylene conversion in the H-OFF zeolites. Furthermore, another OFF application was reported for the catalytic reduction of NO_x by NH_3 using ion exchanged Cu (II) [15,16]. Most recently, Gorshunova et al. [17] studied the K-OFF as a promising adsorbent for capturing hydrocarbons from exhaust gas engines as well as for being useful as a CO_2 storage. Finally, Aponte et al. [18] proposed an additive with an OFF topology for gasoline desulfurization in FCC units. Under these conditions, a selective thiophene adsorption process was observed in the smaller pores (8 rings: $3.9 \times 4.9 \text{ \AA}$).

* Corresponding author.

E-mail address: hdelasa@eng.uwo.ca (H. de Lasa).

The present study proposes the inclusion of Zn in the *OFF* zeolites. These modified zeolites are designated as *a-Zn-OFF* or *b-Zn-OFF* with this designation referring to the different zinc contents used. To the best of our knowledge, there is no previous study on the effect of Zn inclusion in the *OFF* structure. Wang et al. [19] is probably the only study that includes an example of zinc in a zeolite. One should notice however, that a different ZSM5 zeolite was used in Wang et al. [19] study. These authors claim a better zinc dispersion and superior stability, in the modified zeolites (*Zn-ZSM5*).

Regarding the *Zn-OFF*, the present study reports an improvement of the selective sulfur species adsorption properties with Zn inclusion. To demonstrate this, fluidizable particles named as the *Zn-OFF Additive* with a 25 wt% *Zn-OFF* zeolite, 50 wt% inert fused alumina and 25 wt% of Ludox contents were prepared. The *Zn-OFF Additive* was first evaluated using physicochemical characterization. Following this, the enhanced performance of the *Zn-OFF Additives* towards the selective sulfur adsorption was demonstrated in a fluidized CREC Riser Simulator.

The application of the *Zn-OFF Additives* is envisioned for FCC sulfur removal. This approach considers that sulfur species could be adsorbed on the additive with low sulfur left as coke. This reduces as a result, the SO_x formation in the catalyst regenerator, mitigating the overall FCC plant sulfur emissions to the environment.

2. Experimental methods and materials

2.1. Syntheses of Offretite and Zn-Offretite based additives

Three additives were synthesized. Each additive was prepared with three different active materials or zeolites (Offretite, *a*-Zn-Offretite and *b*-Zn-Offretite). Zeolites were mixed with a matrix.

2.1.1. Zeolites: Offretite (OFF), *a*-Zn-Offretite (*a*-Zn-OFF) and *b*-Zn-Offretite (*b*-Zn-OFF)

Three types of zeolites were prepared in this study. All of the zeolites synthesized displayed the *OFF* morphology. The *a-Zn-OFF* and *b-Zn-OFF* zeolites however, were synthesized with the Zn included in the zeolite framework. One should note that the *OFF* preparation procedures of the present study are in line with previous work [20–22]. They differ however, from the ones practiced by others [15–23]. These authors considered metal ions deposited via ion-exchange or metals loaded using incipient wetness.

Fig. 1 reports a summary of the experimental steps followed in the proposed *OFF* synthesis method. First, to synthesize the offretite morphology, a viscous gel solution designated as *Gel 1* was prepared by blending 1.2 g of aluminum hydroxide hydrate, 2.5 g of sodium hydroxide (NaOH, +99%), 1.2 g of potassium hydroxide (KOH, +99%) and 10 g of distillate water for 30 min. This mixture formed a gel as reported in Rx.1 of **Fig. 1**.

Following this, a second gel, designated as *Gel 2*, was prepared with the following components: 60 g of sodium silicate (26.7 wt% SiO_2 , 10.8 wt% Na_2O and 62.5 wt% H_2O) and 14 g of TMA (tetramethyl-ammonium) at a 5 M concentration. This mixture was stirred for 30 min.

Once *Gel 1* and *Gel 2* were prepared, 17 g of *Gel 1* and 74 g of *Gel 2* were blended with the progressive addition of *Gel 2* into *Gel 1*. The resulting solution was kept under high stirring conditions for a 3 h period. On this basis, the *OFF* precursor was obtained with the following expected composition (based on the initial component mixture): 0.08 Al_2O_3 : SiO_2 : 0.51 Na_2O : 0.04 K_2O : 0.25TMA: 14.8 H_2O .

One should note that in spite of having set a 12 $\text{SiO}_2/\text{Al}_2\text{O}_3$ ratio for the *OFF* precursor (*Gel 1* + *Gel 2*) initial components, a practical $\text{SiO}_2/\text{Al}_2\text{O}_3$ ratio of 5 was obtained, as reported later. These findings are in agreement with Moudafi et al. [4] who showed that in order to

achieve a set $\text{SiO}_2/\text{Al}_2\text{O}_3$ ratio, more than double of the $\text{SiO}_2/\text{Al}_2\text{O}_3$ initial component ratios are required.

Furthermore, and to achieve the *OFF* morphology with added zinc, designated in the present study as *Zn-OFF*, the *OFF* synthesis method of **Fig. 1** was modified as follows:

- Zinc nitrate hexahydrate ($\text{Zn}(\text{NO}_3)_2$, reagent grade) in a 10wt% water solution was added drop-by-drop to *Gel 1* (broken line in **Fig. 1**). This formed as a result, a so-called Modified *Gel 1*. The resulting Modified *Gel 1* was intensively blended for 30 minutes, securing in this manner, the expected interaction with the available OH^- solution species.
- Following this, the Modified *Gel 1* was transferred to the *Gel 2* slowly. In addition, an extra 20g of water were added progressively while mixing Modified *Gel 1* and *Gel 2* to avoid precipitation. The above described method was considered for two different $\text{Zn}(\text{NO}_3)_2$ amounts forming two *Zn-OFF* Precursors. The expected formulas established using the initial amounts of zinc, *Gel 1* and *Gel 2* are:
 - a-Zn-OFF Precursor* (based on the initial constitutive component mixture): 0.08 Al_2O_3 : SiO_2 : 0.53 Na_2O : 0.04 K_2O : 0.02 ZnO : 0.25TMA: 20.4 H_2O .
 - b-Zn-OFF Precursor* (based on the initial constitutive component mixture): 0.08 Al_2O_3 : SiO_2 : 0.53 Na_2O : 0.04 K_2O : 0.04 ZnO : 0.25TMA: 20.4 H_2O .

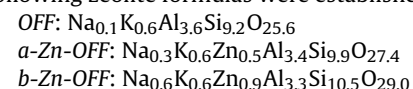
One should mention that the proposed method to prepare the *Zn-OFF Precursor* addresses the following critical issues:

- The value of having Zn^{+2} both in a tetrahedral and square-planar coordination (**Fig. 2**) as primary building units, and these prior to *Zn-OFF Precursor* formation. To accomplish this, a pH of 10 is required. This is achieved using NaOH and KOH with a NaOH/KOH molar ratio of 3.14. This approach is supported by the findings of Stahl et al. [24] and Debiedmme-Chouvy et al. [25] who suggested that high pH concentrations are required for the formation of Zn tetrahedral and Zn square-planar coordination.
- The importance of adding the $\text{Zn}(\text{NO}_3)_2$ solution into the *Gel 1* on a drop-by-drop basis. This is needed to avoid the precipitation of other zinc crystalline phases leading to amorphous materials, which prevent the formation of the *Zn-OFF* precursor.

Following the above described synthesis steps, the *OFF Precursor* with and without Zn was loaded into a 250 ml teflon lined synthesis autoclave. The synthesis autoclave with the *OFF* precursor solution was heated at 160 °C in an oven during 70–90 h. After this, the synthesis autoclave was cooled down to 25 °C. At this point, the formed *OFF* zeolite appeared as a white solid. The zeolite particles were separated by filtration. Following this, they were washed with distillate water until a pH 10 in a filtered liquid was obtained. Once this was achieved, the zeolite particles were dried at 120 °C for 10 h and calcined at 550 °C during 7 h under an air flow. This step allowed one to calcine the TMA, removing it from the *OFF* structure.

A last step in the process of the *OFF* preparation was an ion exchange for sodium removal using an ammonium nitrate solution. This step required zeolite washing using ammonium nitrate as proposed by Hagey [26]. The resulting zeolite was dried at 120 °C and calcined in air at 550 °C during 7 h. This calcination left the *OFF* in a protonated form.

Once all these steps were completed, the quantification of Al_2O_3 , Na_2O , K_2O , SiO_2 components was effected using XRF. On the other hand, Zn content was established using ICP-AES. On this basis, the following zeolite formulas were established:



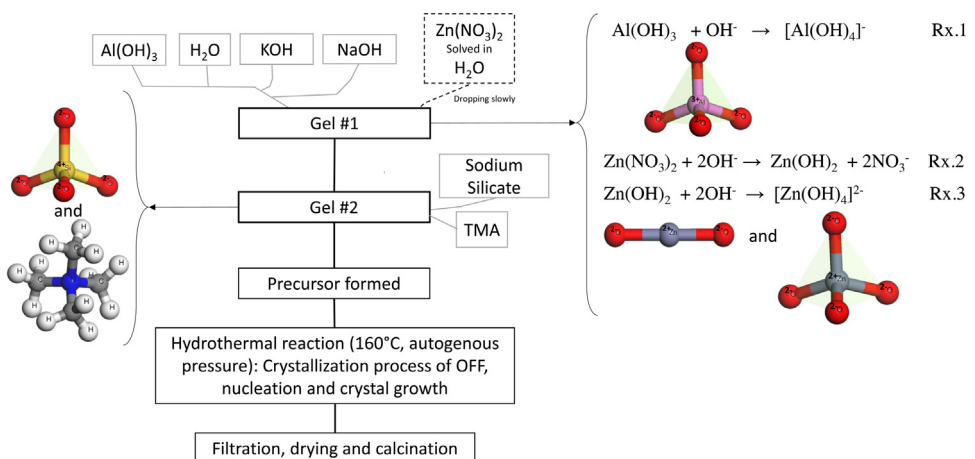


Fig. 1. Schematic description of the OFF and Zn-OFF Zeolite Syntheses. Broken line: reports Zn addition for Zn-OFF zeolite synthesis only. Right hand side: Rx.1) Formation of $[\text{Al}(\text{OH})_4]^-$ unit; Rx. 2–3) formation of $\text{Zn}(\text{OH})_2$ and $[\text{Zn}(\text{OH})_4]^{2-}$ units.

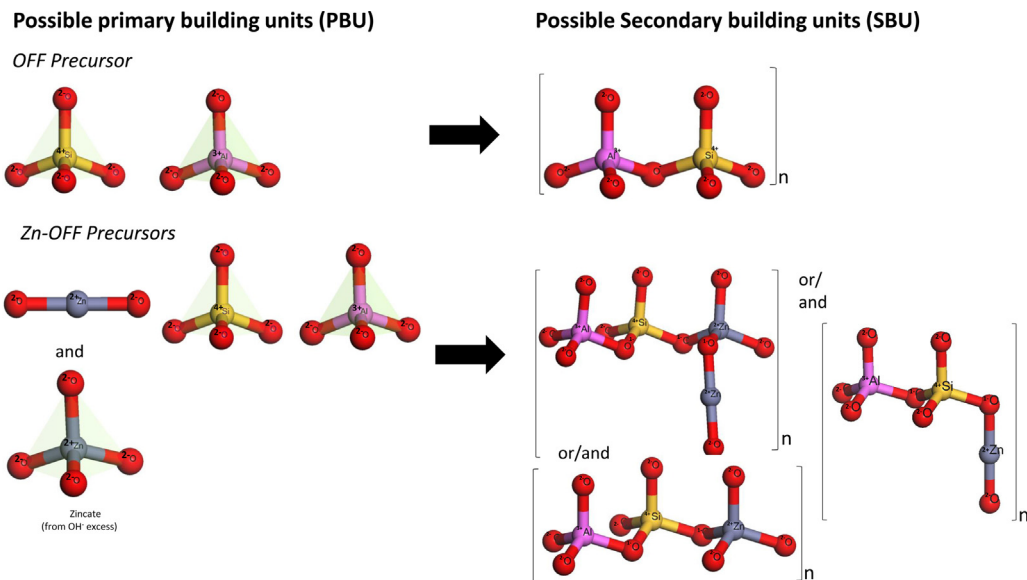


Fig. 2. Building units formed (PBU and PSU) in the OFF and Zn-OFF Zeolites.

The yield of OFF zeolites produced was calculated on the basis of the OFF and Zn-OFF collected. It was observed that a total of 62–87% of aluminum and 53–59% of silicon initial components were incorporated into the OFF structure. In this respect, the modest efficiency reductions were assigned to particles losses during filtration, washing and drying. Moudafi et al. [4] reported similar yield values for the TMA-Offretite synthesis with the incorporation of 50% of silicon. Furthermore, and for both the *a*-Zn-OFF and *b*-Zn-OFF synthesized in the present study, it was noticed that zinc was incorporated into the zeolites structure with a 58–60% yield.

2.1.2. Additives: OFF Additive, *a*-Zn-OFF Additive and *b*-Zn-OFF Additive

Given that the sorbent for thiophenic species in the gasoline range requires fluidizable particles to be implemented in an industrial process, the so-called OFF Additive (pellets) was prepared as follows: (a) 25 wt% of zeolite (Offretite, *a*-Zn-Offretite or *b*-Zn-Offretite), (b) 50 wt% of fused alumina (Aluminum oxide, fused 99%) provided by Sigma-Aldrich as a filler, and (c) 25 wt% of colloidal silica (Ludox AS-40 colloidal silica, 40 wt% suspension in water) from

Aldrich as a binder. The highly viscous resulting slurry was mixed in a mortar forming a homogeneous paste. Then, it was dried at 110 °C for 4 h. Following this, the dried solid cake was calcined at 370 °C for 3 h. Once having completed these steps, the resulting solid was ground and sieved keeping the particles in the 53–100 µm size range for further studies in the CREC Riser Simulator. One should mention that the method followed to manufacture the pellets was similar to the one proposed by Al-Bogami [27] for forming ZSM5 zeolite pellets.

2.1.3. Materials for selective adsorption studies

Thiophene ($\text{C}_4\text{H}_4\text{S}$, Aldrich 99+ % purity) and 2-methylthiophene ($\text{C}_5\text{H}_6\text{S}$, Aldrich 98+ % purity) were used to simulate the gasoline sulfur species while 1,3,5 trimethylbenzene (C_9H_{12} , Sigma-Aldrich 98% purity, Mesitylene) was employed to model the gasoline components. Furthermore, 1.2 wt% of thiophene and 1.2 wt% of 2-methyl-thiophene were employed to establish the selective adsorption of sulfur species using the three additives: a) The OFF Additive, b) The *a*-Zn-OFF Additive and c) The *b*-Zn-OFF Additive.

2.2. Physical and chemical characterization methods

2.2.1. Temperature programmed studies (TPD, TPR and TPO)

The TPD NH₃ analysis was carried out using an AutoChem II 2920 Analyzer from Micromeritics. Samples were pretreated using helium gas for 2 h at 500 °C. Following this, ammonia was adsorbed for 1 h at 100 °C using a NH₃/He gas mixture (4.52% ammonia, 95.58% helium) at a 50.3 STP cc/min. Then, the sample temperature was increased linearly using a 15 °C/min ramp until 580 °C was reached. The resulting desorption peaks were recorded using the instrument thermal conductivity detector (TCD).

Furthermore, and before proceeding to the TPR and TPO analyses, the Zn-OFF zeolites were calcined at 550 °C for 7 h under an air flow. Furthermore, and during the TPR and TPO analyses, the temperature was increased linearly by a 10 °C/min ramp until 680 °C was reached. TPR and TPO used an H₂/Ar gas mixture (9.89% Hydrogen) for zinc oxide reduction and an O₂/He mixture (5.0% Oxygen) for zinc oxidization.

2.2.2. X-Ray diffraction (XRD)

The XRD analysis was effected by using Cu as an anode material, and by using Ni filtered CuK α radiation ($\lambda=0.15406\text{ nm}$) in an Ultima IV X-Ray diffractometer from Rigaku. The XRD analyses were performed in the 5° to 60° of the 2 θ range.

2.2.3. N₂ isotherms

BET was used to evaluate the specific surface area and pore size distribution. Nitrogen adsorption was carried out at 77.818 K using a 3 Flex 3.02 Analyzer Model from Micromeritics. The materials were degassed at 300 °C for 4 h. Nitrogen adsorption covered the 10⁻⁸ to 1 relative partial pressure range.

2.2.4. UV-vis spectra

The UV-vis spectra were obtained using a Shimadzu UV-vis-NIR Spectrometer UV-3600. During the analyses, barium sulphate was used as reflectance standard. The OFF samples were diluted with barium sulphate to obtain a 5 wt% zeolite solid mixture.

2.2.5. Scanning electron microscopy (SEM)

SEM analyses were carried out using a Hitachi S-4500 Field Emission SEM Instrument with a Quartz PCI XOne SSD X-Ray Analyzer. The zeolite crystallites were dispersed using sonication in methanol, with platinum oxide glass used as conductive substrate during SEM analysis.

2.2.6. Fourier transform infrared spectroscopy (FTIR)

FTIR measurements were run in a Bruker IFS55 FTIR Spectrometer with a 4 cm⁻¹ resolution and 100 scans. The samples were diluted with KBr to achieve 50 vol% approximately. The KBr was used to obtain the FTIR spectrum background. Prior to the analysis, samples were saturated with pyridine at 120 °C for one hour using a N₂-pyridine stream. Then, the unbounded pyridine was flushed using a N₂ flow at 120 °C for one hour. After this, the adsorbed pyridine was analyzed using a Diffuse Reflectance Fourier-Transform Infrared Spectrometer (DRIFTS).

2.2.7. Chemical characterizations (XRF and ICP)

The Zn chemical content was determined by using Inductively Coupled Plasma Atomic Emission Spectroscopy at the Biotron at the University of Western Ontario (ICP-AES; Perkin Elmer Optima 3300 Dual View). Al, Si, Fe, and Na contents were established using XRF from a Bruker Analyzer at the Biotron at the University of Western Ontario. Prior to the XRD analysis, all samples were dissolved in aqua regia.

2.3. Reaction system

Experiments were carried out using a CREC Fluidized Riser Simulator [28]. A schematic diagram of a 60 cm³ volume CREC Fluidized Riser Simulator is reported by Aponte et al. [18,29]. This laboratory scale piece of equipment is a bench scale internal recycle batch reactor. This reactor is equipped with an impeller. This impeller induces an upflow of gas, the fluidization of catalyst particles as well as intense gas mixing.

The CREC Riser Simulator operates in conjunction with a vacuum box and a series of sampling valves. These valves allow one to follow a predetermined sequence, the injection of hydrocarbons and the withdrawal of products in short periods of time. Applications of the CREC Riser Simulator in catalytic cracking have been widely reported. Examples are the studies conducted at CREC on the evaluation of zeolites as desulfurization catalysts [18,27,29–32].

2.3.1. Adsorption quantification methods

Sulfur conversions and sulfur balances were established in the CREC Riser Simulator for every run. This was accomplished at the end of every run, by sampling the reactor. Sampling was achieved by connecting the vacuum box to the fluidized reactor. In this respect, two situations were considered:

2.3.1.1. Total product sampling. This total product sampling involves the evacuation and a quasi-total transfer of the products from the CREC Riser Simulator to the vacuum box. This was accomplished by having the vacuum box at approximately 1.6 psi total pressure prior to sampling. At the time that the run was decided to be terminated, the vacuum box and the reactor were connected via the 4 way valve (4PV) until pressure equilibrium between the two vessels was reached. This total product sampling normally takes place in 10–15 s. As a result, and considering pressure and volume differences between these two vessels, it was expected that most of the hydrocarbon species with the only exception of coke, would be transferred from the reactor to the vacuum box (refer to Fig. 3b). These transferred species include all gas phase and adsorbed sulfur species. Thus, the condition of total sampling is equivalent to a first stripping of the OFF Additives.

2.3.1.2. Gas phase product sampling. This involves a partial sampling of the products from the CREC Riser Simulator Reactor. Most of the sampled chemical species belong to gas phase species only. This partial sampling is achieved by having the vacuum box at 39–40 psi, prior to the reactor sampling. The connection of the vacuum box to the reactor via the 4PV, allows under these conditions, a partial transfer of chemical species. There is, as a result, a limited change in total pressure in the reactor. Typically, this gas phase product transfer accounts for 20–30 wt% of all chemical species contained in the CREC Riser Simulator Unit.

Fig. 3a reports an example of gas phase product sampling while Fig. 3b provides an example of total product sampling.

As a result, by using these data, and applying them to the sulfur species in the hydrocarbon mixture, one is able to quantify sulfur species adsorbed on the catalyst (S_{ads}) as follows:

$$S_{ads} = \frac{S_{in} - S_{out,gasphase}}{S_{in}} \times 100 \quad (1)$$

$$S_{in} = X_{injected} m_{injected} \quad (2)$$

$$S_{out,gas phase} = \sum_{i=1}^n X_{i,sp} m_p \quad (3)$$

where S_{in} represents the total sulfur species fed (sulfur species injected as thiophene or 2-methylthiophene) to the reactor, $S_{out,gasphase}$ denotes the sulfur species in the gas phase, $X_{i,sp}$ stands

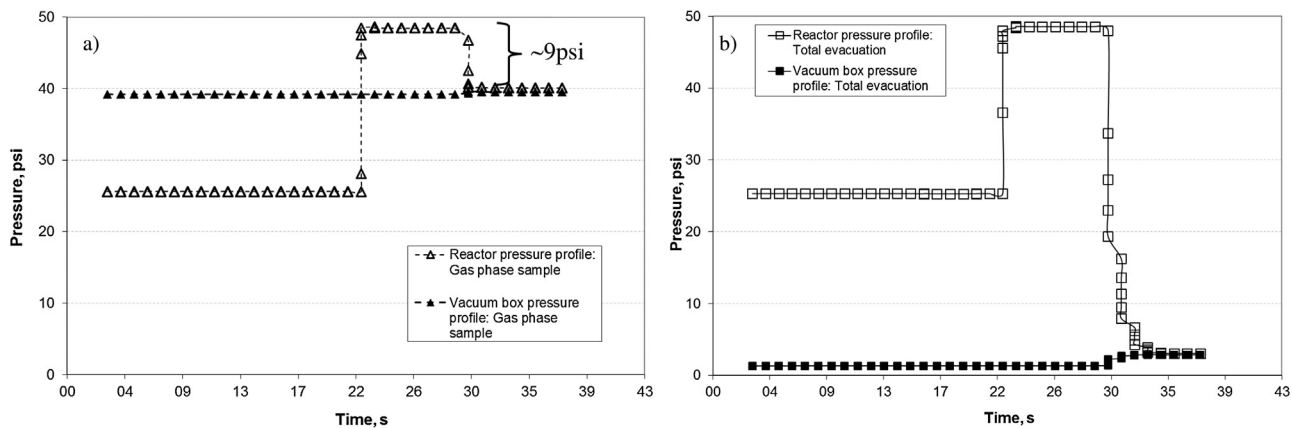


Fig. 3. Pressure profile for a) gas phase sampling (partial evacuation) and, b) reaction total product sampling (quasi-total evacuation). The run condition is for a 0.1 g of b-Zn-OFF additive at 530 °C and 7 s.

for the mass fraction of sulfur species in the gas phase, and m_p is the mass of all chemical species in the gas phase. It is important to mention that the mass of products was determined by calculating the total product moles in the system using the ideal gas law and the average molecular weight of the product mixture on an argon free basis.

Furthermore, the total sulfur balance ($S_{balance}$) was effected for every experiment using the following equation:

$$S_{balance} = \frac{S_{in} - S_{out, total}}{S_{in}} \times 100 \quad (4)$$

where S_{in} is the total sulfur species fed to the reactor as per Eq. (2) and $S_{out, total}$ stands for the sulfur species recovered following the quasi-total evacuation of product species.

Thus, using the described methodology, S_{ads} and $S_{balance}$ can be established for every experimental run. This allows the quantification of the selective adsorption of sulfur species and as result, the evaluation of the performance of all the OFF Additives studied.

2.4. Experimental procedures

Thermal and catalytic runs were performed in the above described CREC Riser Simulator setup. Solid samples of the OFF and Zn-OFF Additives were contacted in this unit, under intense gas mixing, with either thiophene and 2-methylthiophene diluted in 1,3,5-trimethylbenzene. Experimental conditions for the runs were as follows: a) Total initial pressure following the feed injection: 24.5–26.0 psi, b) Temperature: 530 °C, c) Contact time: 7 s, d) additive to oil ratio: 0.6, e) Impeller velocity to secure good fluidization: 5700 rpm. At least 3 repeats for each run were performed to ensure data reproducibility.

Identification and quantification of various chemical species were performed using an Agilent 6890 N Gas Chromatograph (GC) connected to an Agilent 5973 N Mass Selective Detector (MSD). The GC was equipped with two HP-5 dimethylpolysiloxane capillary columns. Each of these columns had a 30 m length, a 0.50 mm nominal diameter and a nominal film thickness of 0.5 μ m. Both columns were connected to the inlet of the GC. One of the columns ended in the Mass Selective Detector (MSD) while the other was coupled to both a Flame Photometric Detector (FPD) and a Flame Ionization Detector (FID).

Thus, each injection into the GC gave three chromatographic signals. The combined information of these three GC analyses allowed both the identification and quantification of hydrocarbons free of sulfur as well as of sulfur containing species. This information was available once the runs were completed. For better GC results, the oven temperature program was run using the following conditions:

a) The oven temperature was initially set to 40 °C for 10 min, b) Following this, the oven temperature was increased at the rate of 8 °C/min up to 70 °C, and c) Finally, once 70 °C was reached, the oven temperature was raised at the rate of 15 °C/min up to 250 °C.

The coke formed on the OFF Additives was measured using a Total Organic Carbon Analyzer (TOCV) with a Solid Sample Module (SSM 5000A) from Shimadzu. TOC for coke analysis was performed once every reaction run was completed, with a total evacuation of the reactor (product phase sampling) as described in Section 2.3.1, point 1. This total evacuation minimized the overexposure of the OFF Additives to hydrocarbons creating a possible bias on coke yield measured.

3. Results and discussion

3.1. Physicochemical characterization

Table 1 summarizes the chemical compositions, NH₃-TPD, pyridine FTIR, BET, micro and macropore area, and pore volume for: a) OFF and Zn-OFF (zeolites), b) OFF and Zn-OFF Additives and c) a Ludox- Fused Alumina Matrix (matrix).

It can be noticed in the last column of **Table 1** that NH₃-TPD and pyridine-FTIR of the matrix additive report no measurable acidity. This demonstrates that the additive matrix used in the OFF and Zn-OFF Additives preparations is inert and does not contribute to its overall sorption performance. This can be later confirmed when comparing the NH₃-TPD for the OFF zeolites with the one for the OFF Additives (**Fig. 4a** and **4b**). One should mention that the Ludox-Fused Alumina Matrix involved in the OFF Additive preparation creates an expected reduction effect on the NH₃-TPD acidity.

Both **Fig. 4a** and **Table 1** report NH₃-TPD results for the three OFF zeolites and OFF Additives. Furthermore, **Table 2** shows both weak and strong sites for all these materials. One can notice that materials with Zn in the structure designated as Zn-OFF show a mild increase in total acidity (1.3 times) as compared to the OFF which free of Zn. It is also observed that the addition of Zn to the OFF structure also leads to an increase in weaker site density (2 times).

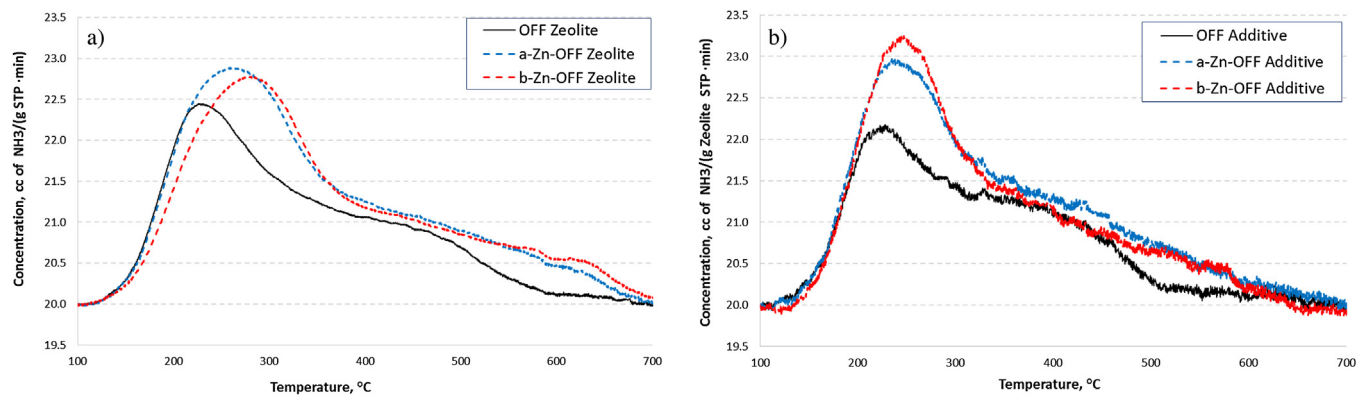
Furthermore, one can also observe in **Fig. 4**, that the NH₃-TPD for the OFF zeolites and that for the Zn-OFF Additives display: a) A close total acidity, b) A displacement of the maximum TPD-NH₃ temperature with Zn content, c) An observed third high temperature peak for both Zn-OFF studied. These third high temperature mild peaks can be associated with dehydroxylation, strong Brønsted and/or Lewis acid sites in zeolites [33,34].

On this basis, one can speculate that the introduction of Zn into the OFF structure promotes a higher diversity of adsorption sites with more variable adsorption bonding strengths. In this respect,

Table 1

Physicochemical properties of the zeolites, additives and matrix.

	OFF		a-Zn-OFF		b-Zn-OFF		Matrix
	Zeolite	Additive	Zeolite	Additive	Zeolite	Additive	
Physicochemical Properties							
Lewis/Bronsted Ratio	0.64	0.68	1.54	1.40	1.59	1.79	0.00
NH ₃ TPD, mmol NH ₃ /g STP at 15 °C/min	1.53	0.36	2.07	0.47	2.00	0.49	0.00
Chemical Composition							
Al ₂ O ₃ , wt%	20.6	67.6	19.3	69.3	18.9	68.6	81.3
SiO ₂ , wt%	58.9	26.7	63.5	25.7	67.5	25.7	16.5
Na ₂ O, wt%	0.59	0.28	1.29	0.42	3.31	1.01	0.20
Fe ₂ O ₃ , wt%	0.06	0.04	0.07	0.04	0.06	0.03	0.03
K ₂ O, wt%	2.02	0.54	2.08	0.51	2.19	0.56	<0.01
Zn, wt%	0.00*	0.00*	1.97	0.55	3.50	1.04	0.00*
Si/Al (mol/mol)	2.42	0.33	2.79	0.31	3.03	0.32	0.17
Al/(Si + Al) (mol/mol)	0.29	0.75	0.26	0.76	0.25	0.76	0.85
Physical properties							
BET Surface Area, m ² /g	430	144	460	183	438	161	19
t-Plot Micropore Area, m ² /g	376	99	408	137	390	115	1
t-Plot External Surface Area, m ² /g	54	45	52	32	48	33	—
Total Volume in Pores, cm ³ /g	0.195	0.113	0.194	0.122	0.185	0.114	0.040

**Fig. 4.** NH₃-TPD spectra for the a) OFF zeolites with and without Zn, and b) OFF Additives with and without Zn (units of concentration in term of zeolite content).**Table 2**TPD-NH₃ results for the zeolites and additives.

	OFF				a-Zn-OFF				b-Zn-OFF			
	Zeolite		Additive		Zeolite		Additive		Zeolite		Additive	
	Temp., °C	mmol NH ₃ /g STP	Temp., °C	mmol NH ₃ /g Zeolite STP	Temp., °C	mmol NH ₃ /g STP	Temp., °C	mmol NH ₃ /g Zeolite STP	Temp., °C	mmol NH ₃ /g STP	Temp., °C	mmol NH ₃ /g Zeolite STP
Weak	227	0.53	223	0.49	258	1.10	241	0.90	274	1.20	242	0.93
Strong	379	1.00	365	0.94	446	0.97	397	0.97	543	0.80	404	1.02

it is speculated that NH₃-TPD peaks in the 200–400 °C range are characteristic of NH₃ chemisorbed on hydroxyl groups in the OFF. Furthermore, the TPD peaks below 200 °C in the zeolites are associated with weakly chemisorbed NH₃ molecules [33].

Regarding the Zn added to the OFF structures (1.97 and 3.50 wt% of Zn), TPR and TPO analyses did not record any measurable hydrogen or oxygen consumption. As a result, it can be hypothesized that the Zn-OFF does not contain any ZnO and/or Zn extra framework crystallites and all the available ZnO and/or Zn are included in the OFF framework.

Fig. 5 reports the characteristic bands for pyridine coordinated on the Lewis sites at 1450 cm⁻¹ and for the protonated pyridine on Bronsted sites at 1545 cm⁻¹. These bands show the relative increase of the Lewis peaks when the Zn is added to the OFF zeolites. One can thus, conclude that the Lewis acidity and the total acidity in the

OFF zeolites with Zn (a-Zn-OFF and b-Zn-OFF) exceeds Lewis acidity of the OFF zeolites without Zn.

Wang et al. [19] reported that having zinc extra framework affects mildly the relative acidity Lewis/Bronsted acidity ratio. These authors observed however, a significant increase in the relative Lewis/Bronsted acidity when Zn was incorporated into the ZSM5 structure. These observations are in good agreement with the findings of the present study, where a speculated incorporation of zinc is accompanied with a significant change in the relative Lewis/Bronsted acidity.

Fig. 6a-c report the XRD for the prepared OFF zeolites before pelletization. One can notice the characteristic X-ray diffraction patterns for the OFF zeolites as reported in the literature [7–10,17,18]. One can also notice that the synthesized OFF are free from the possible erionite or phillipsite contamination.

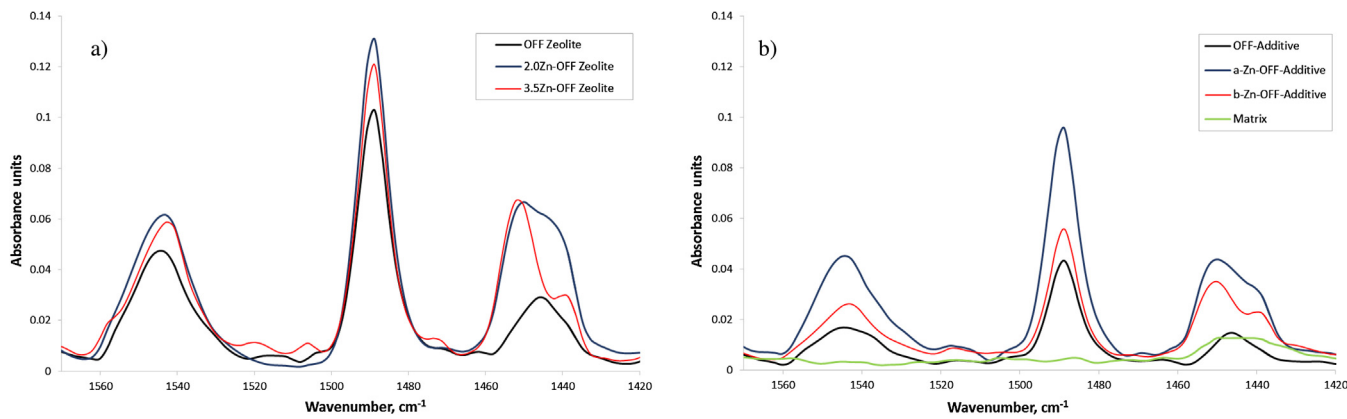


Fig. 5. FTIR spectra for a) active materials (zeolites) and b) additives and Matrix.

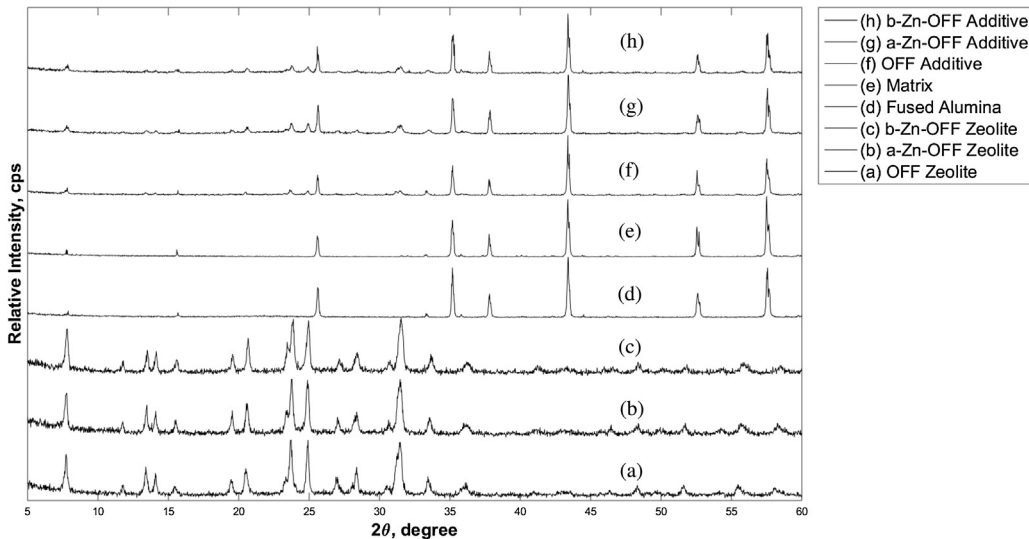


Fig. 6. X-Ray diffraction patterns for the zeolites (a–c), additives (f–h), Matrix (e) and Fused Alumina (d).

Furthermore, one can also see that the addition of Zn (e.g. *a*-Zn-OFF and *b*-Zn-OFF zeolites) shows a XRD pattern very close to that of the pure offretite. The most significant and common peaks for the OFF, the *a*-Zn-OFF and the *b*-Zn-OFF zeolites are located as expected at 7.7°, 23.8°, 24.9° and 31.5° in the 2θ scale. In particular, the peak at 23.8° is consistently the highest, with this being similar to that found in the results of Gorshunova et al. [17], Wang et al. [9] and Quesada et al. [20]. One can notice that no new peaks for ZnO (2θ axis at 31.7°, 34.4°, 36.1°, 56.6°) were observed. This was attributed to two possible causes: a) a low zinc content up to 3.50 wt% in the Zn-OFF, b) the possible absence of sizable extra framework crystallites.

Regarding the OFF, the *a*-Zn-OFF and the *b*-Zn-OFF Additives (see Fig. 6f–g), one can notice that the observable XRD peaks come from the Ludox-Fused Alumina Matrix mainly (Fig. 6d and e). The relatively poor discrimination of the OFF peaks in these diffractograms was assigned to the OFF zeolite dilution when preparing the OFF Additive: a 25w% OFF zeolite in the OFF Additive.

Fig. 7 reports the UV-vis diffuse reflectance spectra for the various OFF zeolites of the present study. Synthesized OFF shows peaks with shoulders at 230 nm and 260 nm. One can observe major differences between the Zn included in the OFF and pure ZnO. The ZnO displays a large adsorption band at 360 nm corresponding to the O²⁻ → Zn²⁺ ligand [19,35]. Therefore, the UV-vis results support a small OFF extra-framework ZnO amount [19].

Table 1 reports N₂ absorption in the synthesized OFF zeolites. Measured BET surface areas for the OFF were 430 m²/g, 460 m²/g and 438 m²/g for the OFF, the *a*-Zn-OFF and the *b*-Zn-OFF, respectively. One can notice in Fig. 8 that the OFF and the Zn-OFF zeolites display an Isotherm Type I without hysteresis. Pore size distribution calculations with the Zn-OFF suggests the advantage of using a slit pore model, with dominant pore sizes in the range of 4–5 Å and 7–8 Å as expected in the OFF.

Fig. 9 reports the morphology of the OFF zeolites with and without Zn. All the zeolites show a similar type of crystallites with a 2–5 µm in length. It appears that the crystallites observed are aggregate rods of hexagonal-shaped crystals. One can also notice that formed crystallites contain parallel formations with core like bundles of small hexagonal rods. It has been reported [36–38] that if: a) Na is included in the zeolite synthesis and b) TMA is used as a synthesis template, the resulting crystallite morphology is very close to the one of the present study. Furthermore, it is also confirmed in Fig. 9b and 9c that the above rod bundle type crystallite morphology do not change with zinc content. This suggests in our view, that zinc is an included species in the OFF structure.

3.2. Adsorption studies

3.2.1. Thermal runs

Thermal cracking runs with no additive loaded involved two blends: a) thiophene (Th) and 1,3,5 trimethylbenzene (TMB) and b)

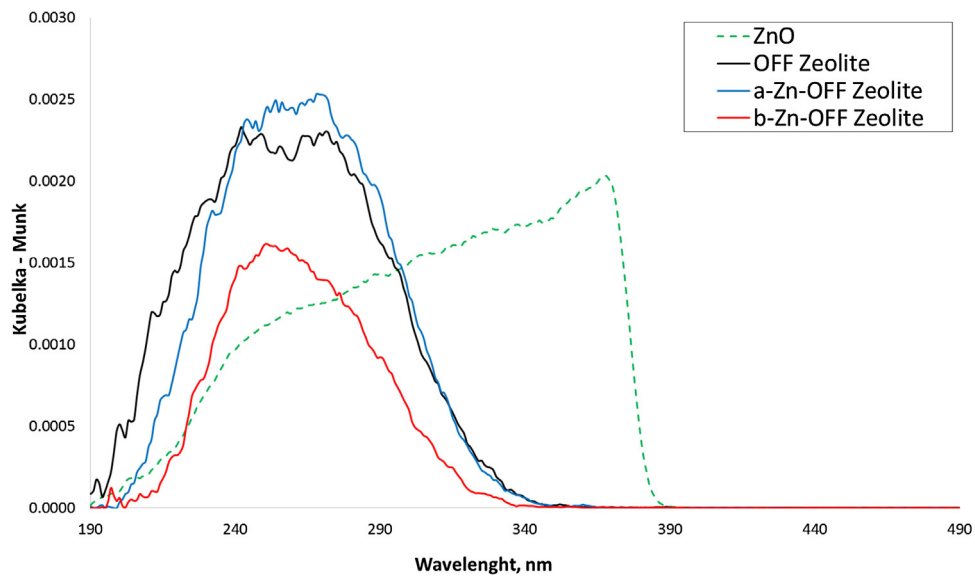


Fig. 7. Diffuse reflectance UV-vis spectra for the OFF, the a-Zn-OFF, the b-Zn-OFF zeolites and the ZnO.

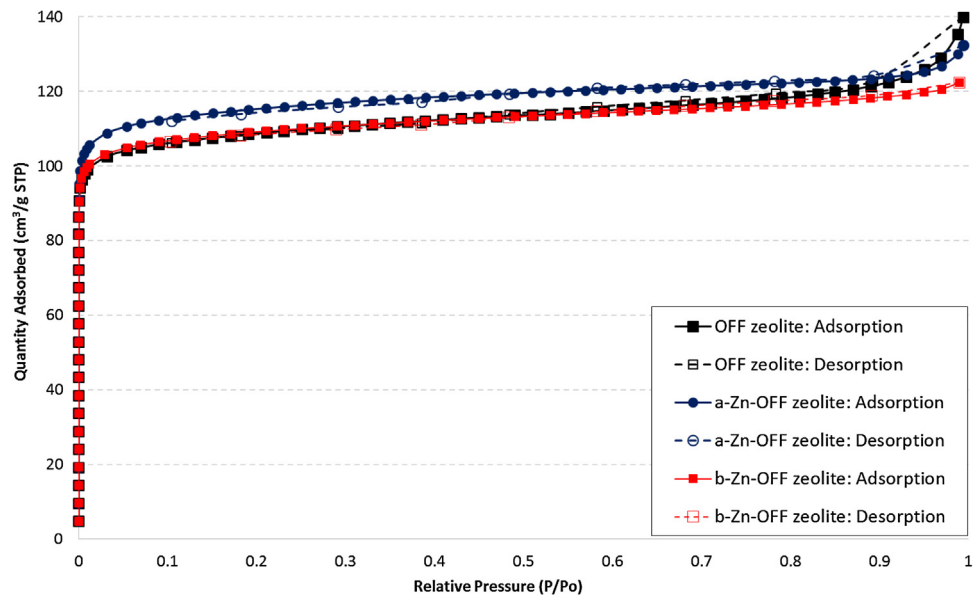


Fig. 8. N_2 Absorption Isotherms at 77.181 K for OFF and Zn-OFF Zeolites.

2-methylthiophene (2MTh) and 1,3,5 trimethylbenzene. Thermal cracking runs with both blends were developed using the CREC Fluidized Riser Simulator unit. No significant Th and 2MTh conversions were observed under the temperature and reaction time studied. TMB conversion was consistently 1–2 wt%. As a result, the thermal runs were considered suitable to demonstrate that there was a very small conversion of the TMB without the OFF Additives. Main products of the TMB conversion were alkylbenzenes (toluene, o- and m-xylene, tetramethylbenzene) and isomers of TMB, resulting likely from disproportionation reactions.

3.2.2. TMB conversions and coke yields

A first step in the present study was to establish the amount of coke produced by both sulfur species and TMB. To clarify this, TMB conversions were measured using both pure TMB and a blend of 2MTh and TMB. Under these conditions, 1.5% and 1.2 wt% of TMB conversion were observed, respectively. It can be noticed that this TMB conversion is very close to the one for the thermal runs. In

particular and for the alkylbenzenes, they were formed in approximately the same amounts as than the TMB converted.

Concerning these results, one can argue that TMB with a critical molecular diameter of 6.89 Å is severely restricted to move in the narrow OFF pores. Thus, TMB cannot access the smallest zeolite inner OFF pores (8 rings: 4.9 Å x 3.6 Å) and available acid sites. As a result, the TMB conversion is severely limited [29] and coke yield becomes insignificant (0.04–0.07 g of carbon/100 g additive).

3.2.3. Zn content effect under thiophenic species adsorption

Fig. 10 reports the calculated S_{ads} and $S_{balance}$ values for the OFF, the a-Zn-OFF, and the b-Zn-OFF Additives using Eq. (1) and Eq. (4).

It can be observed in Fig. 10 that for both S_{ads} and $S_{balance}$ (white and shaded bars), there is a 9 wt% sulfur deficiency in the product species. This consistently missing sulfur (at least 3 repeats per experiment) can only be attributed to the trapped alkylthiophenes remaining in the OFF Additive. One can foresee that there are sulfur species that cannot be removed from the OFF Additive under the

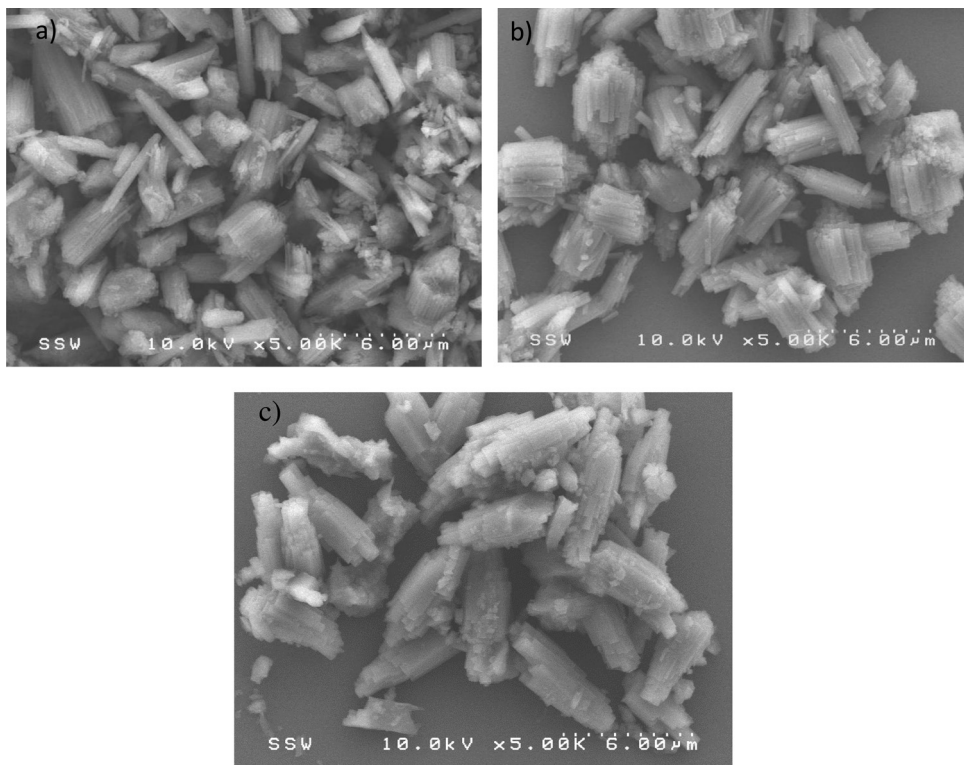


Fig. 9. SEM View of the a) OFF, b) a-Zn-OFF and c) b-Zn-OFF. Note: Reference dimension is 6 μm .

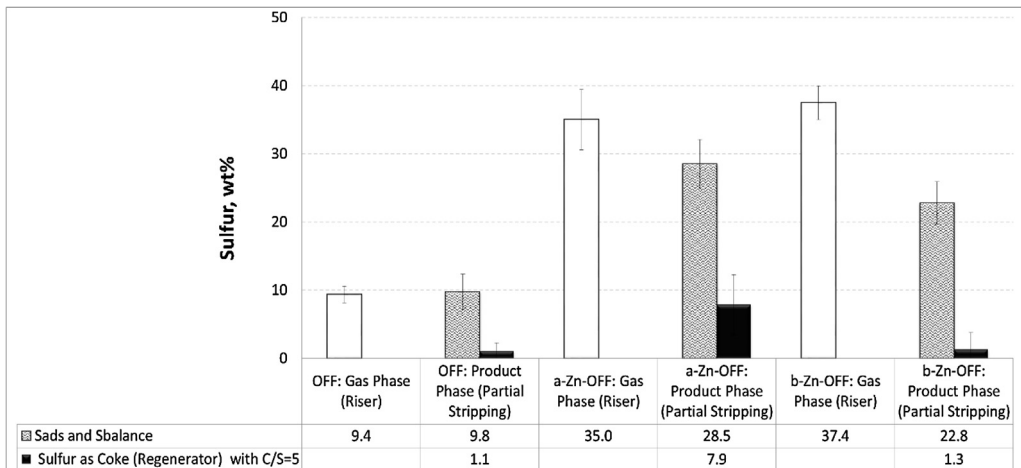


Fig. 10. Sulfur Adsorbed and Balance (S_{ads} and S_{balance}) Calculated with Data from Runs in the CREC Riser Simulator using 0.1 g of Additive and 1.2 wt% of 2MTh in TMB at 530 °C and 7s. Notes: a) Black bars represent sulfur in coke after complete evacuation; b) White bars describe sulfur in the gas phase using Eq. (1) and, c) Shaded bars describe sulfur quantification after quasi-total evacuation using Eq. (4).

1.5–2.0 psi conditions of the CREC Riser Simulator vacuum box during the 10–15 s of evacuation. In fact, a significant fraction of these sulfur species close to 8.7 wt%, requires a second hydrocarbon stripping stage to be removed. This is shown in the TOC analysis of the OFF Additive with 1.1% sulfur content in coke assuming an expected C/S ratio of 5. One should note that the OFF Additive sample analyzed with TOC was collected from the CREC Riser Simulator basket, after a second additional stripping of at least 2–5 min with argon at 530 °C.

Fig. 10 also reports the S_{ads} and S_{balance} parameters for the two Zn-OFF Additives. The S_{ads} which defines the Zn-OFF Additives capability for sulfur species capture, increased to 35.0 and 37.4 wt% levels. This enhanced adsorption capacity due to zinc, as reported in Table 1, can be assigned to the Zn-OFF displaying: a) higher total

acidity, b) higher density of Lewis acid sites, c) stronger site adsorption strength.

Regarding the a-Zn-OFF Additive, the S_{ads} reaches a 35 wt% sulfur capture capacity, while the S_{balance} shows a product deficiency in sulfur of 27.9 wt%. One should notice as well that the sulfur in coke for a C/S of 5, increases to 7.9%. Thus and as a result, the non-stripped sulfur species amount under the initial 1.5–2.0 psi vacuum conditions in the CREC Riser Simulator is 20 wt%. As in the case of the OFF Additive, this 20 wt% can be assigned to trapped alkylthiophenes and can be largely reduced under the second stripping.

Finally, similar trends when using the b-Zn-OFF Additive were observed, with the S_{ads} being 37.4 wt%. However, the b-Zn-OFF Additive yields a S_{balance} deficient by 22.8 wt% only, which suggests a better removal of sulfur adsorbed species under the 1.5–2.0 vac-

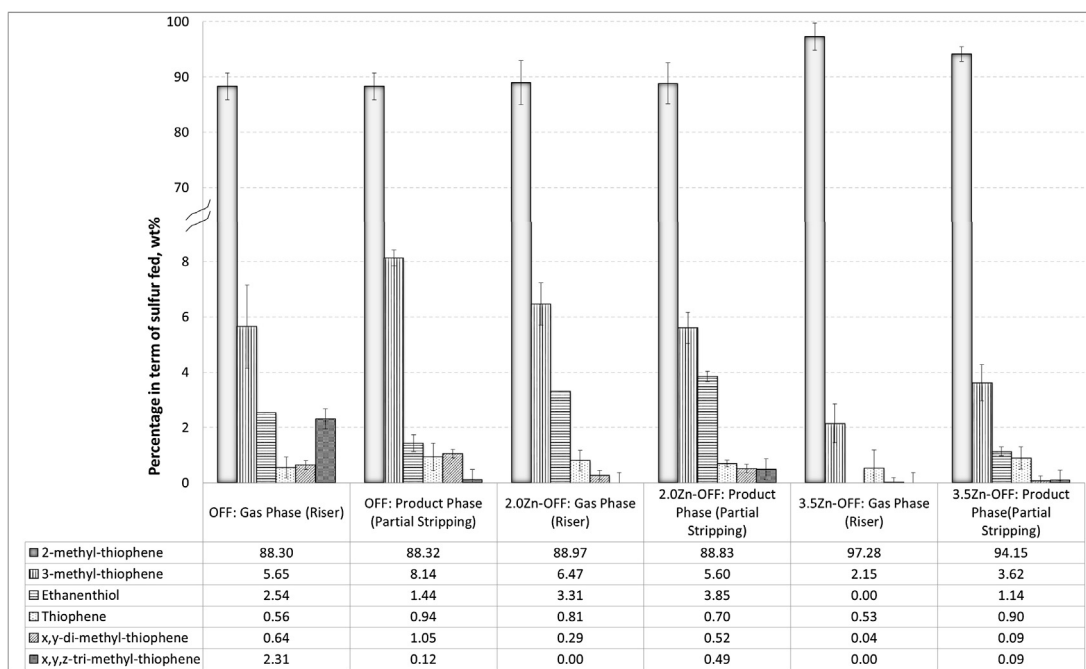


Fig. 11. Distribution of Product Species Containing Sulfur after Runs in the CREC Riser Simulator using 0.1 g of Additive and 1.2 wt% of 2MTh in TMB at 530 °C and 7 s.

uum conditions of the CREC Riser Simulator. In addition, one can notice that if there is a second stripping of hydrocarbons as during the TOC analysis, the sulfur remaining in coke is 1.3% assuming a C/S of 5.

It is thus, anticipated that the *b*-Zn-OFF Additive subject to the most severe stripping conditions as in an FCC plant will lead to the following: a) High sulfur capture, b) low sulfur in coke.

Concerning the reported results, one can hypothesize that surpassing the 1.97% Zn in the Zn-OFF promotes more (Zn-O-Zn)²⁺. These bridges lead to, as shown in Fig. 2, larger acid site (aluminum ions) separation. This modified zeolite structure with increased distance between acid sites promotes sulfur species adsorption rather than sulfur species conversion. This is the case given that alkylation and bimolecular precursor reactions leading to coke are less likely to occur in the *b*-Zn-OFF Additive. In this respect, Penzien et al. [39]; Shubin et al. [40]; Barbosa et al. [41]; Kazansky et al. [42] reported the formation of adjacent aluminum sites, when Zn²⁺ was included as (Zn-O-Zn)²⁺ in the zeolite structure. As a result, one can hypothesize that an increased zinc content in the OFF leads to a higher density of aluminum acid sites placed further apart.

Regarding the OFF, the *a*-Zn-OFF and the *b*-Zn-OFF sorption performances, one should also consider the sulfur species recovered from both the gas phase following evacuation under 1.5–2.0 psi vacuum in the CREC Riser Simulator. Fig. 11 reports in this respect, all the species recovered including the 2-methylthiophene.

Fig. 11 shows consistently and in all cases, that the OFF Additive with and without zinc, yields products with 2MTh and its isomer 3-methylthiophene as the main components. These two chemical species combined represent almost 90 wt% of the sulfur products, with the other product species being thiophene, ethanethiol, dimethylthiophene and trimethylthiophene. Thus, the selective adsorption of the desired species takes place with very limited chemical changes. A similar observation can be made when reviewing the products of the *a*-Zn-OFF and the *b*-Zn-OFF Additives. The 2MTh and 3-methylthiophene continue to dominate the product species with these species being 88–97 wt% of the products. Thus, it can be speculated that adding Zn to the OFF zeolite structure promotes thiophenic selective adsorption, facilitating isomeriza-

tion and alkylation reactions, as a result of the Zn-OFF modified acidity.

Furthermore and in order to establish alkylthiophene species formation, adsorption experiments using the OFF and the Zn-OFF Additives, were developed utilizing Th/TMB blends. Fig. 12 reports both the sulfur adsorption and sulfur balance parameters (S_{ads} and $S_{balance}$) for the OFF and the Zn-OFF Additives. It can be observed that the S_{ads} and $S_{balance}$ display small values in all cases. This is an indication of the low selective adsorption of nonalkylated sulfur species.

Thus, it appears that alkyl groups such as methyl, incorporated into thiophenic molecules play a central role in the promoting of sulfur selective adsorption when using both the OFF and Zn-OFF zeolites. These methyl groups have an inductive effect (electron donating group, base strengthening) in the heteroatomic ring of the 2MTh. Released electrons are transmitted through the heteroatomic ring, towards the S atoms increasing their basicity [43]. These strong bases (electron donors) are more prone to interact with the Lewis acids of the OFF and Zn-OFF zeolites. Fig. 12 also displays a relatively smaller coke formation when *b*-Zn-OFF zeolites are used. This confirms the value of Zn bridges, which facilitate unimolecular reactions instead of bimolecular reactions. The bimolecular reactions are precursor reaction steps for coke formation.

In summary, one can notice that the selective adsorption of alkylated thiophenes on the Zn-OFF Additives, as one can expect in an FCC unit, can lead to the important removal of sulfur species. This happens with very limited coke formation. Thus, thiophenic species in the gasoline boiling point range can be removed in the FCC riser, which prevents their transport to the regenerator. This selective adsorption of sulfur species in the FCC riser prevents their combustion in the regenerator and as a result mitigates SO_x emissions.

4. Conclusions

(a) Zn-OFF Additives with two levels of zinc were synthesized.

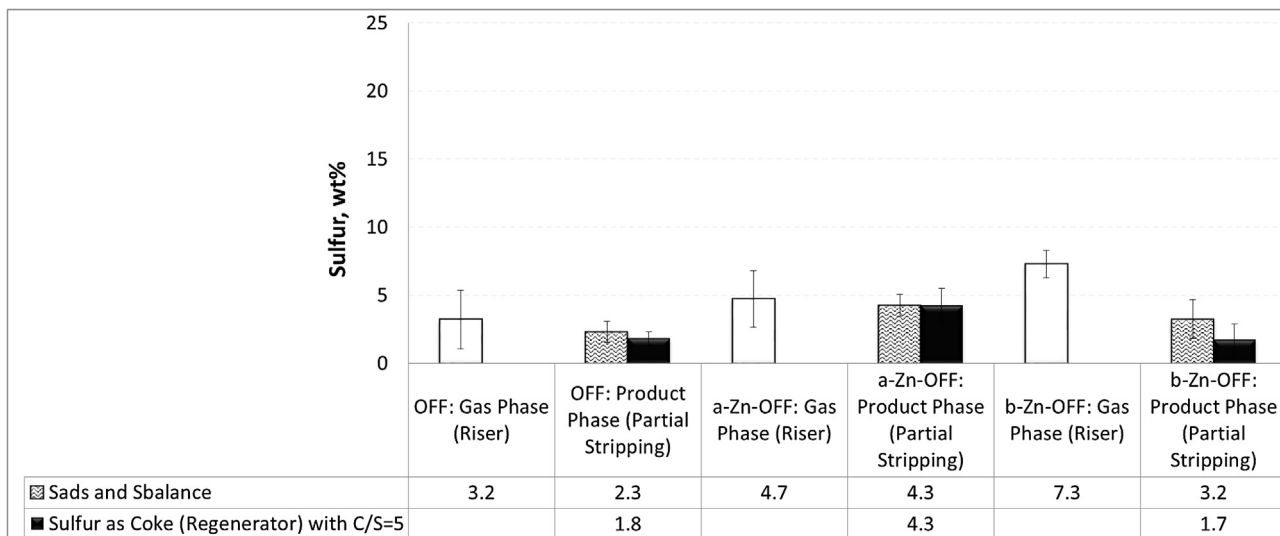


Fig. 12. Sulfur Adsorbed and Sulfur Balance (S_{ads} and $S_{balance}$) Calculated with Data from Runs in the CREC Riser Simulator using 0.1 g of Additive and 1.2 wt% of Th in TMB at 530 °C and 7 s. Notes: a) Black bars represent sulfur in coke after complete evacuation; b) White bars describe sulfur in the gas phase using Eq. (1) and, c) Shaded bars describe sulfur quantification after quasi-total evacuation using Eq. (4).

- (b) Zn was added to the OFF zeolites during the gel synthesis process. It is thought that the prepared Zn-OFF zeolites likely contain most of the zinc species included in the OFF framework.
- (c) The Zn in the OFF zeolites increased the total acidity as well as the acid site strength, with more Lewis acidity being promoted.
- (d) Zn-OFF Additives were prepared using a matrix, in order to have the OFF zeolites as fluidizable particles.
- (e) The Zn-OFF was applied for selective sulfur adsorption removal under FCC conditions. This was tested in a CREC Riser Simulator.
- (f) The selective sulfur adsorption of alkylated thiophenes (e.g. 2MTh) was successfully demonstrated using the Zn-OFF. It was speculated that the Zn-OFF Additives promote unimolecular reactions such as sulfur adsorption rather than bimolecular reactions leading to coke formation.
- (g) The Zn-OFF Additive is a valuable additive given that it can reduce sulfur in catalytic coke, limiting its transport to the catalyst regenerator. As a result, the use of the Zn-OFF Additive can mitigate the SO_x emissions of the entire FCC process.

Acknowledgment

The authors would like to acknowledge the Natural Sciences and Engineering Research Council of Canada (NSERC) and the Ontario Graduate Scholarship (OGS) for the valuable financial support provided to this project. We are also grateful to Dr. Simon Yunez from Micromeritics for the support provided in the additive and zeolite characterization.

Appendix A. . Performance of the b-Zn-OFF Additive Mixed with an FCC Commercial Catalyst

The significant b-Zn-OFF Additive performance reducing sulfur in coke while being mixed with a FCC commercial catalyst was demonstrated using: a) 10 wt% (0.1 g) of the b-Zn-OFF Additive and 90 wt% (0.9 g) of FCC catalyst and b) 100 wt% (0.9 g) of FCC catalyst with no b-Zn-OFF Additive loaded.

The fresh commercial catalyst used was hydrothermally treated (100% steam for 7 h at 750 °C). This treated FCC commercial catalyst had typical properties such as a 136 m²/g of BET surface area and a 84 m²/g of T-Plot surface area.

Table A1

Sulfur in coke for the b-Zn-OFF Additive, the FCC commercial catalyst and the b-Zn-OFF + FCC commercial catalyst blend.

Material	Calculated Sulfur in Coke (wt%)
0.1 g b-Zn-OFF	1.3
0.1 g b-Zn-OFF + 0.9 g FCC Commercial Catalyst	4.5
0.9 g FCC Commercial Catalyst	26.4

Table A1 reports the sulfur in coke for the FCC catalyst and the FCC catalyst mixed with the b-Zn-OFF Additive. The data reported shows that when the FCC catalyst was used with the b-Zn-OFF Additive, the sulfur in coke decreased considerably. This shows the advantage of using the b-Zn-OFF Additive in an FCC process.

References

- [1] M.G. Howden, Zeolites 7 (1986) 255–259.
- [2] M.G. Howden, Zeolites 7 (1986) 260–264.
- [3] S. Yang, N.P. Evmiridis, Microporous Mater. 6 (1996) 19–26.
- [4] L. Moudafi, R. Dutarte, F. Fajula, F. Figueras, Appl. Catal. 20 (1986) 189–203.
- [5] T.E. Whyte, E.L. Wu, G.T. Kerr, P.B. Venuto, J. Catal. 20 (1971) 88–96.
- [6] E.L. Wu, T.E. Whyte, M.K. Rubin, P.B. Venuto, J. Catal. 33 (1974) 414–419.
- [7] C. Fernandez, J.C. Vedrine, J. Grosman, G. Szabo, Zeolites 6 (1986) 484–490.
- [8] A.P. Carvalho, M. Brotas, F. Ramôa, C. Fernandez, J. B-Nagy, E.G. Derouane, M. Guisnet, Zeolites 13 (1993) 462–469.
- [9] Y. Wang, Y. Shang, J. Wu, J. Zhu, Y. Yang, C. Meng, J. Chem. Technol. Biotechnol. 85 (2010) 279–282.
- [10] M. Itakura, Y. Oumi, M. Sadakane, T. Sano, Mater. Res. Bull. 45 (2010) 646–650.
- [11] V. Mavrodinova, C. Minchev, V. Penchev, H. Lechert, Zeolites 5 (1985) 217–221.
- [12] E. Sastre, A. Corma, F. Fajula, F. Figueras, J. Perezpariente, J. Catal. 126 (1990) 457–464.
- [13] P. Dejaive, A. Auroux, P.C. Gravelle, J.C. Védrine, Z. Gabelica, E.G. Derouane, J. Catal. 70 (1981) 123–136.
- [14] G. Bourdillon, R. Pineau, P. Cedex, M. Guisnet, C. Gueguen, Zeolites 6 (1986) 221–224.
- [15] W. Arous, H. Tounsi, S. Djemel, A. Ghorbel, G. Delahay, Stud. Surf. Sci. Catal. 158 (2005) 1883–1890.
- [16] W. Arous, H. Tounsi, S. Djemel, A. Ghorbel, G. Delahay, Top. Catal. 42–43 (2007) 51–54.
- [17] K.K. Gorshunova, O.S. Travkina, G.I. Kapustin, L.M. Kustov, M.L. Pavlov, B.I. Kutepov, Russ. J. Phys. Chem. A 89 (2015) 846–851.
- [18] Y. Aponte, D. Djaouadi, H. de Lasa, Fuel 128 (2014) 71–87.
- [19] L. Wang, S. Sang, S. Meng, Y. Zhang, Y. Qi, Z. Liu, Mater. Lett. 61 (2007) 1675–1678.
- [20] A. Quesada, G. Vitale, US Patent US US2006/246002 A1 (2006).

[21] H. Lechert, in: H. Robson (Ed.), *Verified Syntheses of Zeolitic Materials*, second ed., Elsevier Science B.V., 2001, pp. 33–38.

[22] A. Cichocki, in: H. Robson (Ed.), *Verified Syntheses of Zeolitic Materials*, second ed., Elsevier Science B.V., 2001, pp. 233–235.

[23] N. Chen, W. Garwood, US Patent, 4 (259) (1981) 174.

[24] R. Stahl, R. Niewa, H. Jacobs, *Anorg. Allg. Chem.* 625 (1999) 48–50.

[25] C. Debiemme-Chouvy, J. Vedel, M.-C. Bellissent-Funel, R. Cortes, *J. Electrochem. Soc.* 142 (1995) 1359–1364.

[26] H. Hagey, The University of Western Ontario, Dissertation, 1997.

[27] S.A. Al-Bogami, The university of western Ontario, Dissertation (2013).

[28] H. de Lasa, U.S. Patent 5 (102) (1992) 628.

[29] Y. Aponte, The University of Western Ontario, Dissertation, 2011.

[30] S. Al-Bogami, H. de Lasa, *Fuel* 108 (2013) 490–501.

[31] H. de Lasa, R. Hernandez, G. Tonetto, *Ind. Eng. Chem. Res.* 45 (2006) 1291–1299.

[32] L. Jaimes, M. Badillo, H. de Lasa, *Fuel* 90 (2006) 2016–2025.

[33] B.M. Lok, B.K. Marcus, C.L. Angell, *Zeolites* 6 (1986) 185–194.

[34] F. Lonyi, J. Valyon, *Micropor. Mesopor. Mat.* 47 (2001) 293–301.

[35] S. Bordiga, C. Lamberti, G. Ricchiardi, L. Regli, F. Bonino, A. Damin, A. Zecchina, *Chem. Commun.* 5 (2004) 2300–2301.

[36] L. Moudafi, P. Massiani, F. Fajula, F. Figueras, *Zeolites* 7 (1987) 63–66.

[37] M.L. Occelli, R.A. Innes, S.S. Pollack, J.V. Sanders, *Zeolites* 7 (1987) 265–271.

[38] J.F. Bengoa, S.G. Marchertti, N.G. Gallegos, A.M. Alvarez, M.V. Cagnoli, A.A. Veramian, *Ind. Eng. Chem. Res.* 36 (1997) 83–87.

[39] J. Penzien, A. Abraham, J. Van Bokhoven, A. Jentys, T.E. Müller, C. Sievers, J. Lercher, *J. Phys. Chem. B* 108 (2004) 4116–4126.

[40] A.A. Shubin, G.M. Zhidomirov, V.B. Kazansky, R.A. Van Santen, *Catal. Lett.* 90 (2003) 137–142.

[41] L. Barbosa, A. Santen, *J. Phys. Chem. C* 111 (2007) 8337–8348.

[42] V.B. Kazansky, A.I. Serykh, E.A. Pidko, *J. Catal.* 225 (2004) 369–373.

[43] M. Smith, in: *Organic Synthesis*, third ed., Elsevier Inc., United State, 2010, pp. 77–217.